Published OnlineFirst August 17, 2015; DOI: 10.1158/0008-5472.CAN-15-0986

Molecular and Cellular Pathobiology

Cancer Research

Enhanced Chemokine Receptor Recycling and Impaired S1P1 Expression Promote Leukemic Cell Infiltration of Lymph Nodes in Chronic Lymphocytic Leukemia

Laura Patrussi[1,2], Nagaja Capitani[1,2], Veronica Martini[3,4], Marco Pizzi[5], Valentina Trimarco[3,4], Federica Frezzato[3,4], Filippo Marino[5], Gianpietro Semenzato[3,4], Livio Trentin[3,4], and Cosima T. Baldari[1,2]

Abstract

Lymphocyte trafficking is orchestrated by chemokine and sphingosine 1-phosphate (S1P) receptors that enable homing and egress from secondary lymphoid organs (SLO). These receptors undergo rapid internalization and plasma membrane recycling to calibrate cellular responses to local chemoattractants. Circulating chronic lymphocytic leukemia (CLL) cells display an abnormal increase in the surface levels of the homing receptors CCR7 and CXCR4 concomitant with low S1P receptor 1 (S1P1) expression. In this study, we investigated the role of receptor recycling on CXCR4/CCR7 surface levels in CLL cells and addressed the impact of quantitative alterations of these receptors and S1P1 on the ability of leukemic cells to accumulate in SLOs. We show that recycling accounts, to a major extent, for the high levels of surface CXCR4/CCR7 on CLL cells. In addition, increased expression of these receptors, together with S1P1 deficiency, is detectable not only in circulating leukemic cells, but also in SLOs of CLL patients with lymphoadenopathy. We further provide evidence that ibrutinib, a Btk inhibitor that promotes mobilization of leukemic cells from SLOs, normalizes the imbalance between CXCR4/CCR7 and S1P1. Taken together, our results highlight the relevance of chemokine and S1P receptor recycling in CLL pathogenesis and clinical outcome. *Cancer Res; 75(19); 4153–63. ©2015 AACR.*

Introduction

Lymphocyte homing is regulated by chemokine receptors that respond to stromal ligands (1, 2). The main B-cell homing receptors are CCR7 and CXCR4, which promote their entry into secondary lymphoid organs (SLO), where CXCR5 takes over for their follicular traffic (3, 4). Leukemic cells exploit this process to acquire proliferation and survival cues, as exemplified by chronic lymphocytic leukemia (CLL; refs. 5, 6). CLL cells express increased surface CXCR4/CCR7 and CXCR5, which favors their bone marrow and SLO homing and their positioning close to CXCL13-secreting stromal cells, respectively (7, 8). The defective expression in these cells of the egress S1P receptor S1P1 may further contribute to the retainment of CLL cells in the prosurvival stromal niche (9, 10).

The plasma membrane chemokine receptor pool is highly dynamic, undergoing downmodulation in the presence of high ligand concentrations and recycling when these decrease, allowing for a rapid adjustment of the surface levels without overall quantitative changes (11). Here we investigated the role of recycling in the regulation of the surface levels and chemotactic response of the homing receptors CXCR4 and CCR7. We further asked whether the quantitative CXCR4/CCR7 and S1P1 alterations correlate with the ability of CLL cells to accumulate in these tissues. We show that efficient recycling contributes to maintaining high surface CXCR4/CCR7 in CLL cells and that increased expression of these receptors, together with S1P1 deficiency, is present not only in circulating CLL cells, but also in lymph nodes and bone marrow. We also show that ibrutinib, a Btk inhibitor that promotes leukemic cell mobilization from SLOs, restores the balance between homing and egress receptors by reciprocally modulating CCR7 and S1P1 expression, underscoring the pathologic relevance of this imbalance in CLL.

Materials and Methods

Patients and healthy donors

Peripheral blood samples were collected from 52 patients satisfying standard morphologic and immunophenotypic criteria for CLL. B cells from 18 buffy coats were used as controls of the adult healthy population. Informed consent was obtained according to the Declaration of Helsinki. At the time of collection,

[1]Department of Life Sciences, University of Siena, Siena, Italy. [2]Istituto Toscano Tumori, Siena, Italy. [3]Venetian Institute of Molecular Medicine, Padua, Italy. [4]Department of Medicine, Hematology and Clinical Immunology Branch, Padua University School of Medicine, Padua, Italy. [5]Surgical Pathology and Cytopathology Unit, Department of Medicine, University of Padua, Padua, Italy.

Note: Supplementary data for this article are available at Cancer Research Online (http://cancerres.aacrjournals.org/).

L. Patrussi and N. Capitani contributed equally to this article.

Corresponding Author: Cosima T. Baldari, Department of Life Sciences, University of Siena, Via Aldo Moro 2, Siena 53100, Italy. Phone: 3905-7723-4400; Fax: 3905-7723-4476; E-mail: baldari@unisi.it

doi: 10.1158/0008-5472.CAN-15-0986

Published OnlineFirst August 17, 2015; DOI: 10.1158/0008-5472.CAN-15-0986

patients had never received treatment. For 5 patients, blood samples were collected before and after a 4-month ibrutinib treatment with a fixed daily dose of 420 mg, administered orally on a continuous schedule. Experiments were approved by the local Ethics Committee.

B cells were purified by negative selection using the RosetteSep B-cell enrichment Cocktail (StemCell Technologies) followed by density gradient centrifugation on Lympholite (Cedarlane Laboratories).

Antibodies and reagents

Antibodies against CXCR4 (Abcam), CCR7 (clone Y59 Novus Biologicals), actin (Millipore), and pVav (Y160; Invitrogen), and secondary peroxidase-labeled antibodies (Amersham Pharmacia Biotech) were used for immunoblot. Anti-CXCR4 (clone 12G5), CCR7 (clone 150503; R&D Systems), and anti-EDG1/S1P1 (Novus Biologicals) antibodies were used for flow cytometry. Anti-CXCR4 and CCR7 (Abcam), Rab5 (BD Biosciences), Rab7 and Rab11 (Santa Cruz Biotechnology) were used for immunofluorescence. Secondary Alexa Fluor 488- and 555-labeled antibodies were from Invitrogen. Human CXCL12 and CCL21 and fibronectin were from Sigma-Aldrich and rhICAM-1/Fc from R&D Systems.

Activations and immunoblots

Cells were starved for 2 hours in RPMI–1% BSA and activated at 37°C with 500 ng/mL CXCL12 or CCL21 (Sigma-Aldrich). For immunoblots, cells were lysed in 1% Triton X-100, 20 mmol/L Tris-HCl (pH 8), 150 mmol/L NaCl added with protease inhibitors (Invitrogen). Postnuclear supernatants were processed for immunoblot as described (12).

RNA purification and quantitative RT-PCR

RNA was extracted from B cells from healthy donors and CLL patients and retrotranscribed as described (13). Real-time

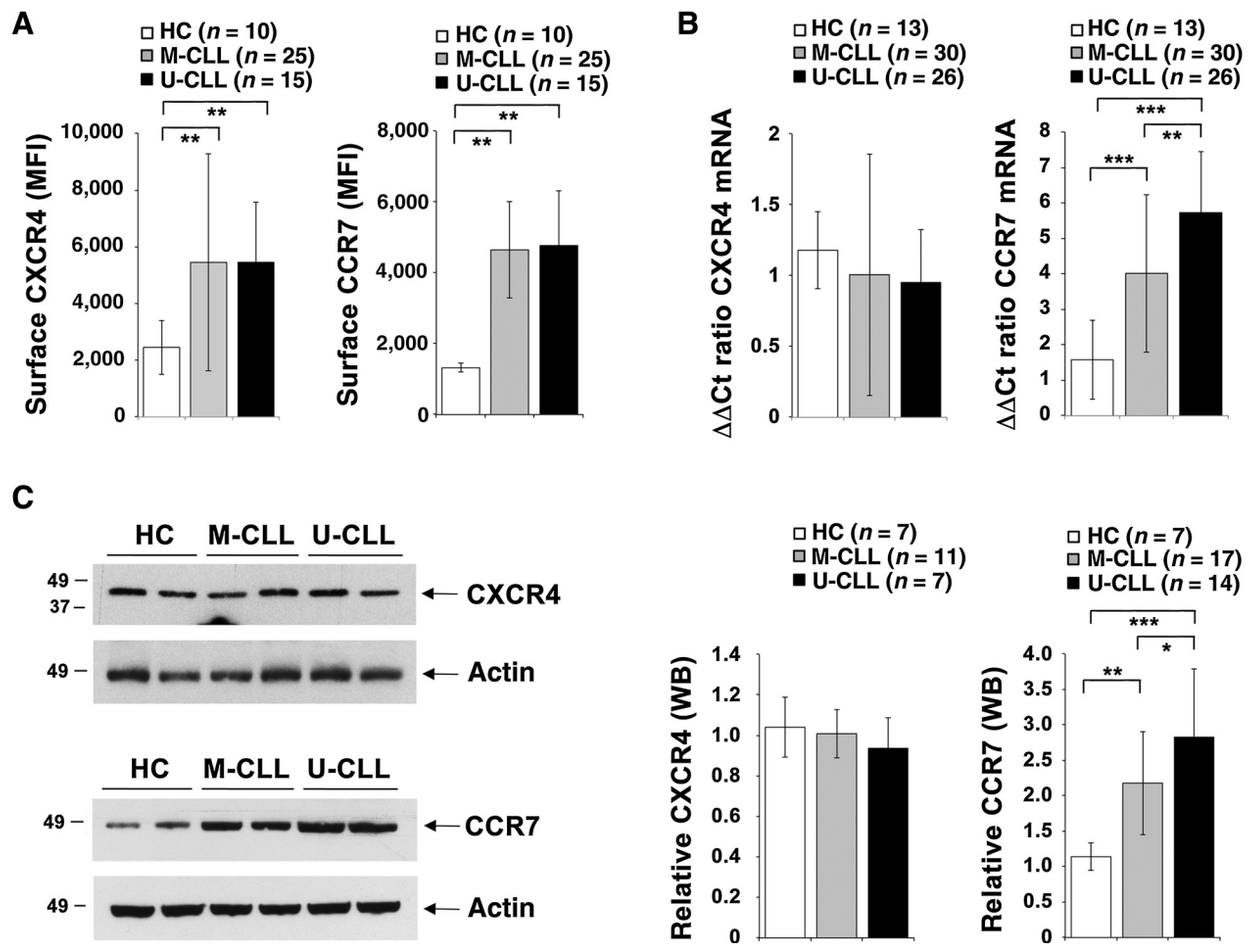

Figure 1.

The increase in surface CXCR4/CCR7 on CLL cells is only partly accounted for by increases in total protein and mRNA levels. A, flow cytometric analysis using fluorochrome-conjugated mAbs of surface CXCR4 (left) or CCR7 (right) on whole fresh blood samples from healthy donors (HC) and M-CLL or U-CLL patients (MFI±SD). B, qRT-PCR analysis of CXCR4 (left) or CCR7 (right) mRNA in purified HC, M-CLL, or U-CLL B cells. The relative gene transcript abundance was determined on triplicate samples using the $\Delta\Delta C_t$ method (mean normalized fold expression ±SD). C, immunoblot analysis of CXCR4/CCR7 expression on cell lysates from purified HC, M-CLL or U-CLL B cells. Left, representative immunoblots. Right, quantification (mean±SD) of CXCR4/CCR7 expression normalized to actin. *, $P < 0.05$; **, $P < 0.01$; ***, $P < 0.001$. For each donor/patient, the results of the flow cytometry, real-time RT-PCR and immunoblot showed the same trend. The data presented in A and B were analyzed using the Mann–Whitney rank sum test.

Published OnlineFirst August 17, 2015; DOI: 10.1158/0008-5472.CAN-15-0986

PCR was performed in triplicate on 96-well optical PCR plates (Sarstedt AG) using SSo Fast EvaGreen SuperMix (Bio-Rad Laboratories) and a CFX96 Real-Time System (Bio-Rad Laboratories). Results were processed and analyzed using Bio-Rad CFX Manager v1.5 software (Bio-Rad). Transcript levels were normalized to HPRT1 or ACTB. Primers used for amplification are listed in Supplementary Materials and Methods.

Flow cytometry

Flow cytometric analysis of surface CXCR4/CCR7 was carried out using fluorochrome-conjugated mAbs or isotype controls on fresh whole blood samples. To quantitate the ratio of surface to total CXCR4/CCR7, B cells were purified, fixed, and, where required, permeabilized using the Cytofix/Cytoperm plus kit (BD Biosciences). The fixation protocol resulted in a decrease in surface labeling (Supplementary Fig. S1), accounting for the lower mean fluorescent intensities (MFI) measured under these conditions as compared with measurements on fresh whole blood samples. Flow cytometry was carried out using a Guava Easy Cyte (Millipore) or FACSCanto (BD Biosciences) cytometer. Before S1P1 staining, cells were resuspended in serum-free medium added with 0.5% fatty acid–free BSA (Sigma-Aldrich) and incubated for 30 minutes at 37°C to allow recycling of intracellular receptors. Data were analyzed and plotted using Flowjo (Tree Star Inc).

Immunofluorescence microscopy and colocalization analyses

Cells were processed for immunofluorescence microscopy as described (14). Confocal microscopy was carried out on a Zeiss LSM700 using a 63× objective as described (14). The quantitative colocalization analysis of CXCR4 or CCR7 and Rab protein signals

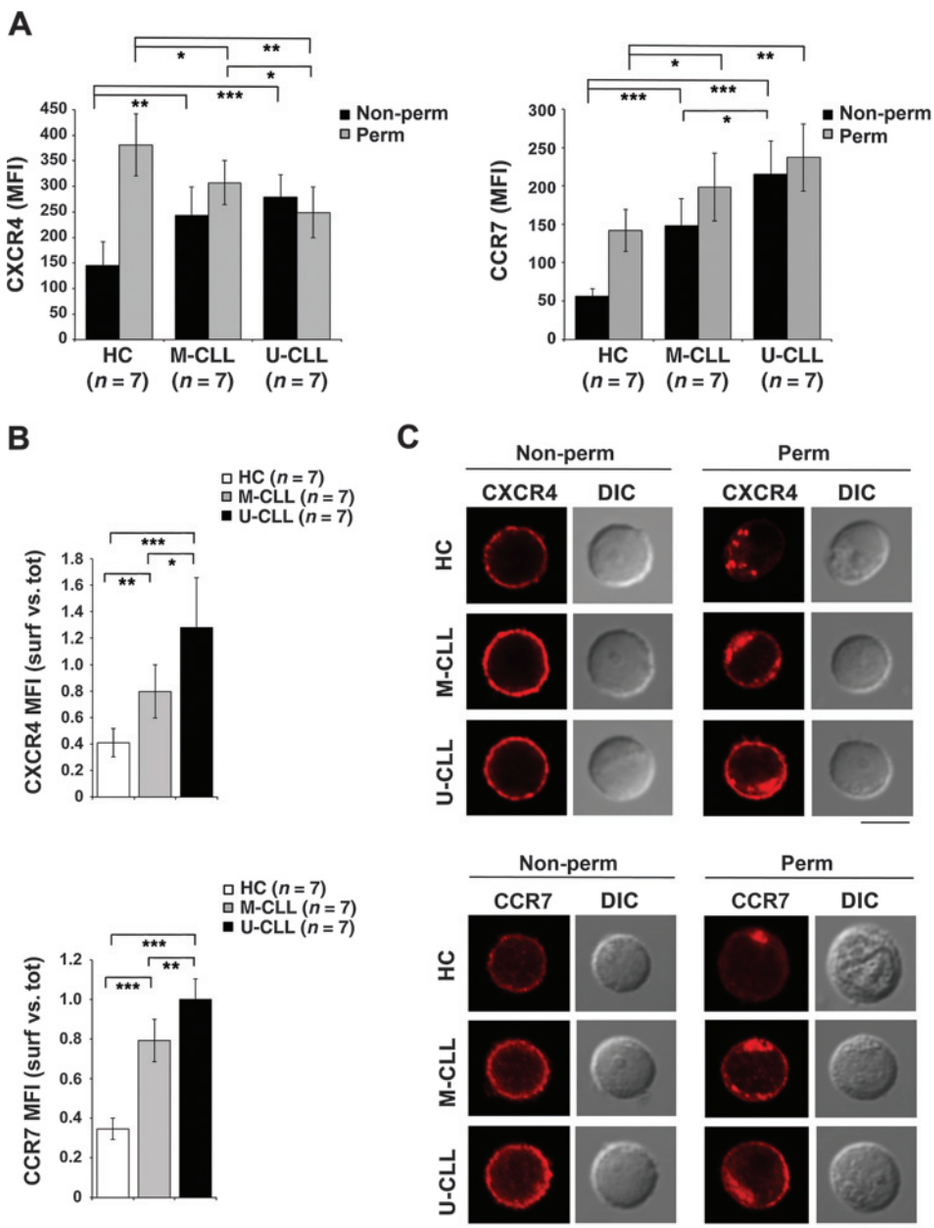

Figure 2.
An imbalance between plasma membrane and endosomal pools contributes to the increased surface CXCR4/CCR7 in CLL cells. A, flow cytometric analysis using fluorochrome-conjugated mAbs of CXCR4 (left) or CCR7 (right) on purified HC, M-CLL, or U-CLL B cells, either nonpermeabilized or permeabilized (MFI±SD). B, ratio of surface to total MFI of CXCR4 (top) and CCR7 (bottom) from HC, M-CLL, or U-CLL B cells. Data are expressed as ratio (mean±SD) of MFI in nonpermeabilized cells (surface) to permeabilized cells (total). *, $P < 0.05$; **, $P < 0.01$; ***, $P < 0.001$. C, immunofluorescence analysis of purified HC, M-CLL, or U-CLL B cells either nonpermeabilized or permeabilized and labeled for CXCR4 (top) or CCR7 (bottom). Median optical sections are shown. Size bar, 5 μm.

Published OnlineFirst August 17, 2015; DOI: 10.1158/0008-5472.CAN-15-0986

was performed on median optical sections using ImageJ and JACoP plug-in to determine Manders' coefficient (15).

Flow cytometry and immunofluorescence analysis of receptor recycling and cell adhesion and polarization

CXCR4/CCR7 recycling following antibody-dependent down-regulation was quantitated by flow cytometry as described (16, 17). To analyze recycling by immunofluorescence, cells were equilibrated 30 minutes at 37°C in RPMI–1% BSA, incubated with saturating concentrations of specific antibodies or 100 ng/mL CXCL12/CCL21 at 37°C for 40 minutes, permeabilized, and processed for immunofluorescence microscopy. CXCL12/CCL21 treatment did not interfere with binding of the anti-CXCR4/CCR7 antibodies (Supplementary Fig. S2).

Adhesion assays on rhICAM-1/Fc (R&D Systems)- or fibronectin (Sigma-Aldrich)-coated plates in the presence or absence of 100 ng/mL CXCL12/CCL21 were carried out as described (12). Cells were stained with TRITC-labeled phalloidin and polarization analyzed by immunofluorescence microscopy as described (12).

Chemotaxis assays

Chemotaxis assays were carried out using 24-well Transwell chambers with 5-μm pore size polycarbonate membranes (Corning Life Sciences, Schiphol-Rijk, The Netherlands) as described (18).

Immunohistochemistry

CCR7, S1P1, and CXCR4 immunohistochemical expression was assessed on matched lymph node and bone marrow samples from 5 CLL cases (2 M-CLL, 3 U-CLL). Three tonsils with reactive follicular hyperplasia were used as controls. Immunohistochemistry was performed on 4 μm thick FFPE sections. Heat/citrate-based antigen retrieval methods were applied, as described (19). Antigen detection was performed with the Bond Polymer Refine Detection kit in an automated immunostainer (Bond maX).

Receptor expression was assessed according to the anatomical compartment (T-cell and B-cell zones for reactive tonsillar tissue; proliferation centers and small cell areas for CLL).

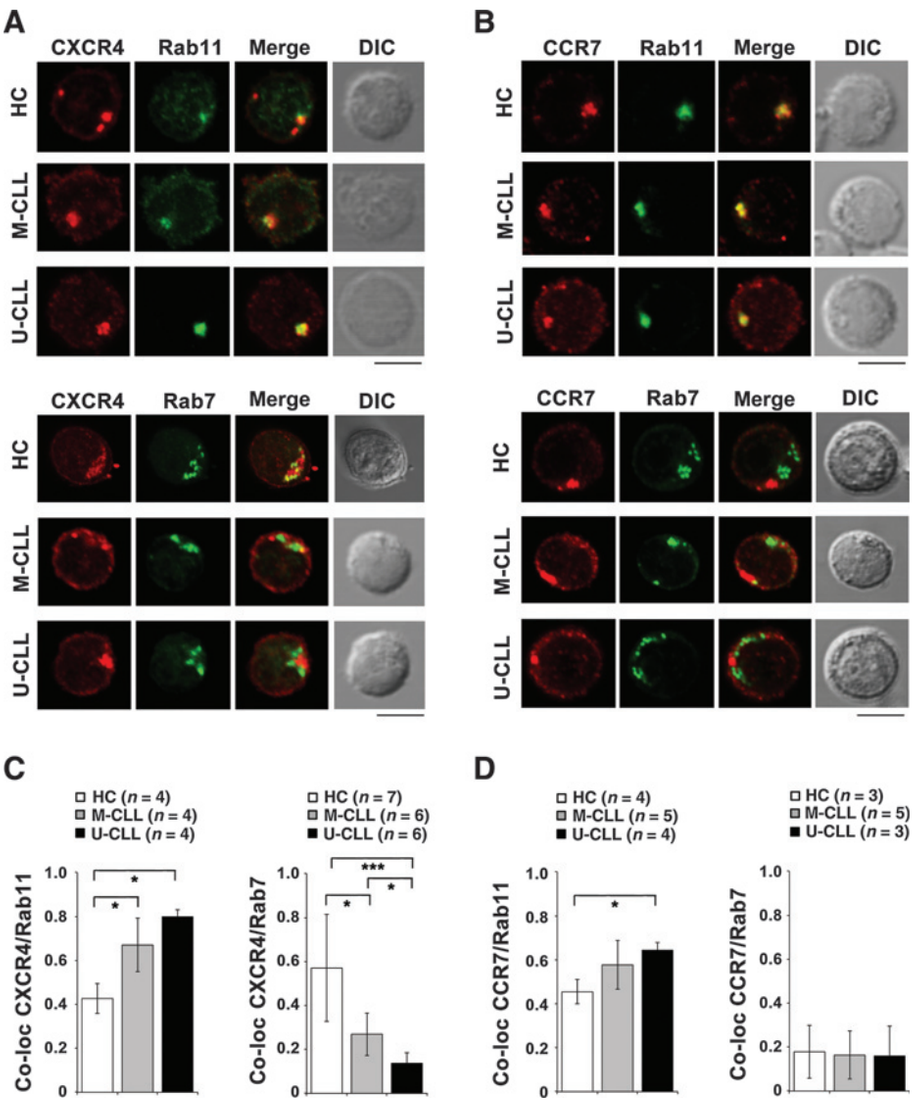

Figure 3.
Enhanced CXCR4/CCR7 sorting to recycling endosomes in CLL B cells. A and B, immunofluorescence analysis of Rab11 (green, top) or Rab7 (green, bottom) and either CXCR4 (red; A) or CCR7 (red; B) in purified HC, M-CLL, or U-CLL B cells incubated with 100 ng/mL of CXCL12/CCL21 at 37°C for 40 minutes, fixed, and permeabilized. Representative median optical sections are shown. Size bar, 5 μm. C and D, quantification using Manders' coefficient of the weighted colocalization of $CXCR4^+$ (C) or $CCR7^+$ (D) vesicles with the $Rab11^+$ and $Rab7^+$ compartments in individual medial confocal sections (mean ± SD; ≥20 cells/marker). *, $P < 0.05$; **, $P < 0.01$; ***, $P < 0.001$.

Published OnlineFirst August 17, 2015; DOI: 10.1158/0008-5472.CAN-15-0986

Statistical analyses

Mean values, SD values, and the Student *t* test (unpaired) were calculated using the Microsoft Excel application. The Mann–Whitney rank sum test was also used for small samples (<5 data points) or if the population was not normally distributed. A level of $P < 0.05$ was considered statistically significant.

Results

An alteration in the balance between plasma membrane and endosomal CXCR4/CCR7 pools contributes to their increased surface levels in CLL cells

CXCR4/CCR7 expression was measured on peripheral B cells from CLL patients and healthy controls. Based on the *IGHV* mutational status, patients were divided into two groups, with mutated (M-CLL) and unmutated (U-CLL) *IGHV* (20, 21). Flow cytometric analysis showed that, as reported (7), the surface levels of CXCR4/CCR7 were increased in CLL cells compared with healthy B cells (Fig. 1A).

To understand whether this reflects an increase in the total cellular content, CXCR4/CCR7 expression was measured by real-time RT-PCR and immunoblot. At variance with the increased surface CXCR4 levels in CLL cells, the respective mRNA levels were comparable with healthy controls (Fig. 1B). Consistent with our previous report (9), CCR7 expression was enhanced in CLL cells, with significant differences between U-CLL and M-CLL (Fig. 1B). These results were confirmed by immunoblot (Fig. 1C). As CXCR4/CCR7 are stored in part in recycling endosomes (11), this suggests that the ratio between the surface and intracellular receptor pools may be altered in CLL cells, at least for CXCR4.

To address this issue, CXCR4/CCR7 were measured by flow cytometry in intact and permeabilized normal and CLL B cells. Expression of both receptors was significantly higher when measured on permeabilized normal B cells (Fig. 2A), indicating that a substantial proportion of CXCR4/CCR7 is intracellular. In contrast, the levels of CXCR4/CCR7 were comparable in intact and permeabilized CLL cells (Fig. 2A and B), indicating that the bulk of CXCR4/CCR7 is associated with the plasma membrane. This was confirmed by immunofluorescence analysis, which showed a less substantial endosomal CXCR4/CCR7 staining in CLL cells compared with normal B cells (Fig. 2C). Of note, the ratio of surface to total receptor was not only consistently higher in CLL cells when compared with normal B cells, but also significantly higher in U-CLL versus M-CLL cells (Fig. 2B). Collectively, these results suggest that plasma membrane transport of CXCR4/CCR7 may be more efficient in CLL cells.

Enhanced receptor recycling contributes to the increased surface CXCR4/CCR7 levels on CLL cells

To assess the fate of CXCR4/CCR7 following their internalization at the plasma membrane, normal and CLL B cells were treated with CXCL12/CCL21 and stained with antibodies to the respective receptor. Cells were costained for makers of recycling (Rab11) or late (Rab7) endosomes, to which they are alternatively sorted from early endosomes. Normal B cells showed a partial CXCR4 colocalization with Rab11 (Fig. 3A and C). Consistent with its preferential late endosomal sorting following internalization (22), CXCR4 also partially colocalized with Rab7 (Fig. 3A and C). This did not apply to CCR7 (Fig. 3B and D), which is preferentially sorted to recycling endosomes (23) and that indeed showed a strong colocalization with Rab11 (Fig. 3B and D). The vesicular CXCR4 pool, which was less prominent in CLL cells, showed a lower Rab7 colocalization and a higher Rab11 colocalization compared with normal B cells (Fig. 3A and C), indicating that internalized receptors are sorted to recycling rather than late endosomes in CLL cells. An increase in CCR7 colocalization with Rab11 was also observed (Fig. 3D). Similar results were obtained when receptor internalization was induced using specific mAbs (Supplementary Fig. S3). These results suggest that the increased proportion of surface CXCR4/CCR7 in CLL cells is likely accounted for by a more efficient recycling. Indeed, CLL cell treatment with colchicine, which inhibits recycling by targeting the microtubule cytoskeleton, results in a decrease in surface CXCR4/CCR7 (Supplementary Fig. S4).

To directly address this issue, CXCR4/CCR7 recycling was measured by flow cytometry. Initial experiments on normal B cells showed that CXCL12/CCL21 treatment resulted in the rapid mobilization of the respective intracellular receptor pools to the plasma membrane (Supplementary Fig. S5), thereby interfering with the analysis of CXCR4/CCR7 undergoing ligand-dependent internalization. We therefore used an antibody-based assay to selectively track receptors that had been engaged at the plasma membrane (16). The kinetics and extent of CXCR4/CCR7 internalization in CLL cells were comparable with normal B cells (Fig. 4A). At variance, CXCR4/CCR7 recycling were strongly enhanced in CLL cells, with significant differences between M-CLL and U-CLL (Fig. 4B). Hence, CLL cells can effectively recycle their homing receptors.

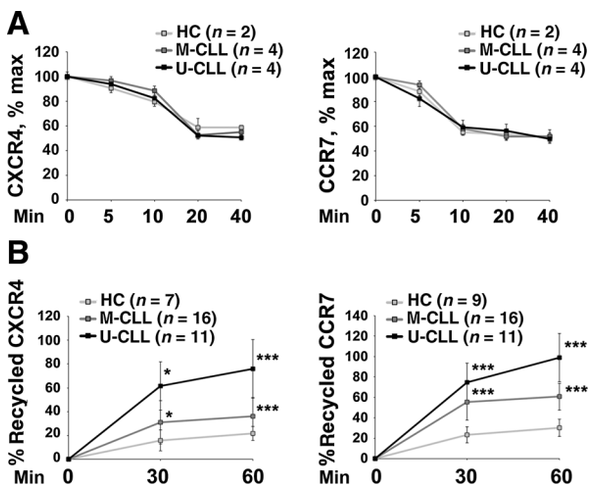

Figure 4.

CLL B cells effectively recycle CXCR4 and CCR7. A, flow cytometric analysis of CXCR4 (left) and CCR7 (right) downregulation in HC, M-CLL, or U-CLL B cells incubated with anti-CXCR4 or anti-CCR7 antibodies for 30 minutes on ice, washed, incubated at 37°C for the indicated times and labeled with fluorochrome-conjugated secondary antibodies. B, flow cytometric analysis of CXCR4/CCR7 recycling in purified HC, M-CLL, or U-CLL B cells. Cells were incubated for 30 minutes on ice with receptor-specific mAbs, washed, shifted to 37°C for 40 minutes, then subjected to acid stripping (time 0), and incubated for the indicated times at 37°C. Receptor:antibody complexes that had recycled to the cell surface were measured by labeling with fluorochrome-conjugated secondary antibodies. Data are presented as percentage of internalized receptors that recycled to the cell surface. Error bars, SD. *, $P < 0.05$; ***, $P < 0.001$.

Published OnlineFirst August 17, 2015; DOI: 10.1158/0008-5472.CAN-15-0986

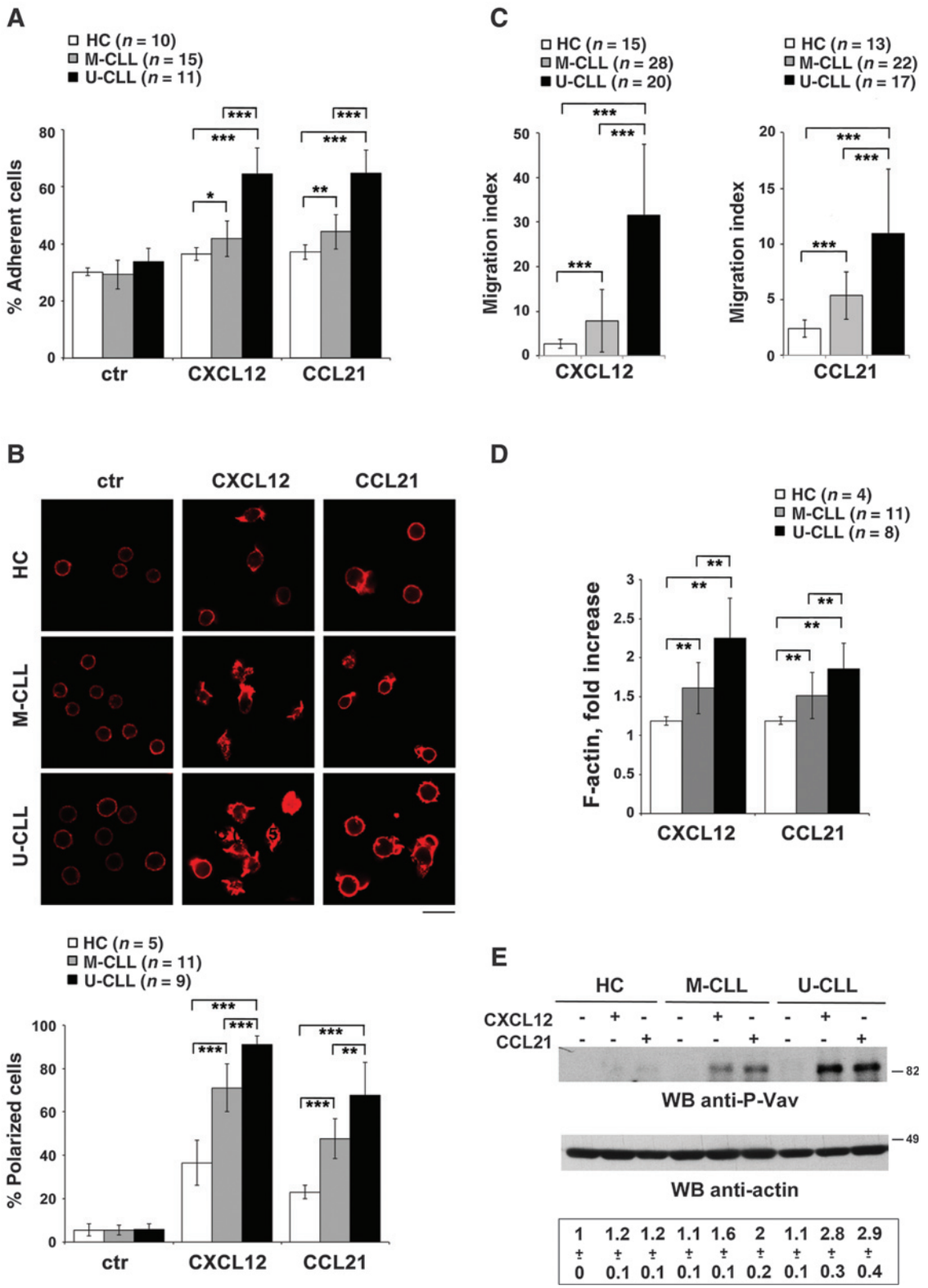

Published OnlineFirst August 17, 2015; DOI: 10.1158/0008-5472.CAN-15-0986

Abnormally high surface CXCR4/CCR7 levels translate into robust chemotactic responses of CLL cells

To understand whether the increase in surface CXCR4/CCR7 in CLL cells translates into quantitative differences in the cellular response, the outcome of CXCR4/CCR7 engagement was investigated by analyzing the main steps that coordinate B-cell homing. CXCR4/CCR7-dependent adhesion to ICAM-1 was strongly enhanced in U-CLL cells, with significant differences also compared to M-CLL cells (Fig. 5A). A small, yet significant enhancement was also observed for M-CLL cells (Fig. 5A). Similar results were obtained when cells were plated on fibronectin (Supplementary Fig. S6).

Following CXCL12/CCL21-dependent adhesion to ICAM-1, B cells morphologic changes associated with F-actin reorganization, resulting in their polarization (Fig. 5B). The proportion of polarized cells was increased for both M-CLL and U-CLL cells as compared with healthy controls (Fig. 5B). Analysis of CXCL12/CCL21-dependent migration showed that M-CLL cells had more robust chemotactic responses compared to normal B cells, with a further increase in U-CLL cells (Fig. 5C).

These results suggest that CXCR4/CCR7 signaling to the actin cytoskeleton is enhanced in CLL cells. Quantification of F-actin staining in control and CLL B cells plated on ICAM-1 and stimulated with CXCL12/CCL21 showed increased levels of actin polymerization in CLL cells, with the highest levels in U-CLL (Fig. 5D). Moreover, CXCL12/CCL21-dependent phosphorylation of Vav, a Rho GTPase GEF that promotes actin reorganization in hematopoietic cells (24) was enhanced in CLL cells (Fig. 5E). Hence, the CXCR4/CCR7-dependent response in CLL cells correlates with their increased surface levels.

Imbalance in homing and egress receptor expression in SLOs and BM from CLL patients

Taken together with the S1P1 expression defect in U-CLL cells (ref. 9 and data not shown for the patients who participated in this study), the increase in surface CXCR4/CCR7 in circulating CLL cells suggests that these alterations may impact on leukemic cell transit through SLOs and bone marrow. Nonetheless, surface CXCR4/CCR7 can undergo dynamic changes in the presence of local chemokine gradients (25, 26). Moreover, under certain conditions their expression is shut off to overcome responsiveness to T-cell zone chemokines (27). The fate of CXCR4/CCR7 in CLL cells accumulating in SLOs and bone marrow is unknown. We carried out an immunohistochemical analysis of CXCR4, CCR7, and S1P1 on lymph node and bone marrow biopsies from CLL patients, using tonsillar tissue as control.

In normal lymphoid tissue, CCR7 was expressed in B-cell and T-cell zones, with the highest positivity on centrocytes and centroblasts in secondary follicle germinal centers (GC; Fig. 6A and B). Membrane positivity was coupled with cytoplasmic expression, consistent with the two pools in circulating B cells (Fig. 6B). CXCR4 expression closely resembled that of CCR7, with moderate-to-strong expression in GCs and low-to-absent staining in mantle zones (Fig. 6E and F). Unlike CCR7/CXCR4, S1P1 was selectively expressed in mantle zone cells (Fig. 6I), with both membrane and cytoplasmic positivity (Fig. 6J). High-endothelial vein endothelial cells were also S1P1-positive. Within GCs, scattered positivity was solely observed in histiocytes/accessory cells (Fig. 6J).

Immunohistochemical analysis of CLL lymph node biopsy samples showed strong CCR7 (Fig. 6C and D) and CXCR4 (Fig. 6G and H) positivity in small lymphocytes and paraimmunoblasts of proliferation centers. Consistent with the S1P1 expression defect in both U-CLL cells and cells from M-CLL patients with lymphoadenopathy (9), lymph nodes were S1P1-negative (Fig. 6K and L). CCR7 and S1P1 expression did not differ between matched lymph node and bone marrow biopsy samples (Supplementary Fig. S7). Hence, CXCR4/CCR7 expression remains high on CLL cells following their SLOs and bone marrow accumulation generating, together with the S1P1 expression defect, an imbalance that is expected to promote lymphoadenopathy.

Ibrutinib treatment reverses the homing/egress receptor imbalance in CLL by reciprocally modulating CCR7 and S1P1 expression

Clinical trials have identified ibrutinib, a Btk inhibitor that suppresses both BCR and chemokine receptor survival signaling during leukemic cell transit through SLOs and bone marrow, as an effective alternative to current chemoimmunotherapy-based regimens (28–31). A striking effect of inbrutinib is the rapid lymph node shrinkage paralleled by a transient lymphocytosis (28). We hypothesized that this could result from a normalization of the homing and egress receptor imbalance. CLL cells were treated with ibrutinib, and the mRNA and surface levels of CXCR4, CCR7, and S1P1 were quantitated. Ibrutinib treatment resulted in a robust upregulation in surface S1P1 (Fig. 7A), paralleled by a modest, yet significant, downregulation in surface CCR7. No effect on CXCR4 was observed (Fig. 7A). These results were confirmed by real-time RT-PCR (Fig. 7B).

Figure 5.

Enhanced chemotactic responses to CXCL12/CCL21 in CLL B cells. A, quantification by flow cytometry of the percentage of purified HC, M-CLL, or U-CLL B cells that adhered to rhICAM-1/Fc-coated wells following 10-minute treatment with 100 ng/mL CXCL12/CCL21. The data, which refer to quadruplicate samples from each donor/patient, are presented as percentage of input cells that remained attached to each well. B, quantification of the percentage of polarized HC, M-CLL, or U-CLL B cells plated for 5 minutes on rhICAM-1/Fc-coated slides, stimulated for 5 minutes with 100 ng/mL CXCL12/CCL21, and labeled with Phalloidin-TRIC. The percentage of polarized versus nonpolarized cells was calculated on 4 wide-field images/well. Representative images are shown. Size bar, 10 μm. C, migration of purified HC, M-CLL, or U-CLL B cells measured after 3-hour treatment with 100 ng/mL CXCL12/CCL21. The data, obtained on duplicate samples from each donor/patient, are presented as mean migration index (ratio of migrated cells in chemokine-treated vs. untreated samples) ± SD. D, quantification of actin polymerization in purified HC, M-CLL, or U-CLL B cells plated for 5 minutes on rhICAM-1/Fc-coated slides and stimulated for 5 minutes with 100 ng/mL CXCL12/CCL21. Slides were labeled with Phalloidin-TRIC. The data, calculated on four wide-field images from each donor/patient, are presented as phalloidin MFI in stimulated vs. unstimulated samples, quantitated using ImageJ and normalized to the intracellular actin content. See B for representative images. E, immunoblot analysis with an anti–phospho-Vav antibody of postnuclear supernatants from a representative healthy donor (HC) and CLL patient with mutated (M-CLL) or unmutated (U-CLL) *IGHV*, either unstimulated or stimulated for 1 minute with 100 ng/mL CXCL12 or CCL21. The control anti-actin immunoblot of the stripped filter is shown below. The migration of molecular mass markers is indicated. The quantification below is calculated on 5 HC, 3 M-CLL, and 5 U-CLL. Error bars, SD. *, $P < 0.05$; **, $P < 0.01$; ***, $P < 0.001$. Statistics were carried out using Student *t* test, with the exception of the data presented in D, for which the Mann–Whitney rank sum test was used.

Published OnlineFirst August 17, 2015; DOI: 10.1158/0008-5472.CAN-15-0986

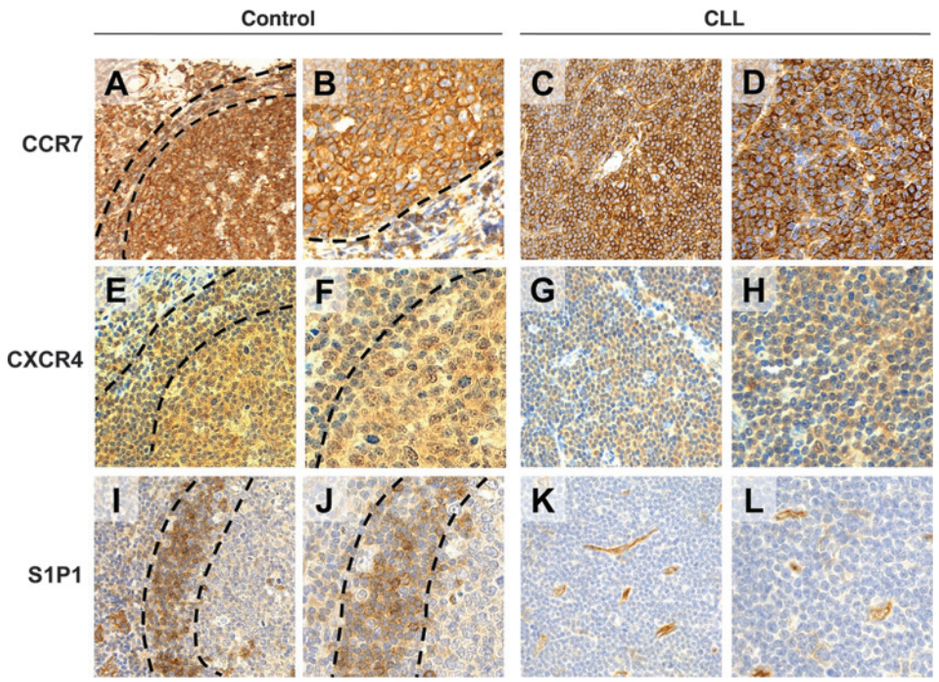

Figure 6.
CCR7 and CXCR4 and S1P1 expression in normal reactive lymphoid tissue and CLL lymph nodes. In non-neoplastic lymphoid tissue, CCR7/CXCR4 were expressed in both B-cell and T-cell areas (A and E), with stronger immunohistochemical positivity in secondary follicle GCs (B and F; dotted lines, mantle zone). S1P1 expression was restricted to mantle zone B-lymphocytes (I and J). Malignant CLL lymphocytes were $CCR7^{+}$ (C and D) and $CXCR4^{+}$ (G and H). No differences were observed between small lymphocytes and paraimmunoblasts of proliferation centers. Neoplastic cells were consistently S1P1-negative (K and L; positive internal control; intramural vessels; immunoperoxidase staining; original magnification, ×10 and ×20).

The analysis was extended to leukemic cells from patients undergoing ibrutinib treatment. Cells were analyzed before the start of treatment and after 4 months of daily ibrutinib administration. Consistent to the *in vitro* results, *in vivo* ibrutinib treatment resulted in a significant upregulation of S1P1 expression, with a concomitant reduction in CCR7 but no effect on CXCR4 (Fig. 7C and D). Hence ibrutinib targets the homing and egress receptor imbalance likely by modulating the expression of the respective genes.

Discussion

Increased surface CCR7/CXCR4 on CLL cells correlates with both lymphoadenopathy and disease stage (7, 32, 33) and translates into enhanced *in vitro* migration (32, 34, 35), as also documented in this report. Here we identify recycling as a central mechanisms exploited by CLL cells to increase the surface levels of these receptors. The absence of significant alterations in the mRNA or protein CXCR4 levels demonstrates indeed that the increase in surface CXCR4 on CLL cells results from their enhanced ability to recycle this receptor. Although CCR7 expression is enhanced in CLL as compared with normal B cells, the increase in its surface pool in leukemic cells indicates that this also applies to CCR7.

The trafficking pathways of internalized CXCR4/CCR7 differ, CCR7 being preferentially sorted to recycling endosomes (36) and CXCR4 to lysosomes (37, 38), as also supported by our colocalization analyses. Our data show that these pathways are dysregulated in CLL cells. The plasma membrane receptor pool is indeed significantly higher in CLL compared with normal B cells, concomitant with an increase in their recycling endosome association that is particularly striking for CXCR4, which in CLL cells shows a significantly more limited association with late endosomes compared with normal B cells. It is worth emphasizing that the abnormality in CCR7/CXCR4 recycling and the resulting alterations in the chemotactic response, while displayed by CLL cells independently of the *IGHV* mutational status, is more severe in U-CLL cells. This may contribute to the high incidence of lymphoadenopathy in these patients.

Taken together with the reciprocal alterations in CCR7 and S1P1 expression, the recycling-related increase in surface CCR7/CXCR4 on circulating CLL cells suggests a scenario where homing to SLOs and bone marrow is favored and egress therefrom prevented. The immunohistochemical analysis of CCR7/CXCR4 in CLL lymph node biopsies, showing that leukemic cell maintain high the receptor levels at this location, indicates that CLL cells have indeed the potential to generate a sustained and robust response to the stromal ligands. This is expected not only to promote leukemic cell survival but also their lymphoid niche retention, particularly when the negativity of these cells for S1P1, shown here and consistent with a recent report (39), is taken into account. Other abnormalities affecting the migratory ability of CLLs are likely to further exacerbate this imbalance, particularly in U-CLL patients, including alterations in the expression of CXCR5, CD38, CD49d, CD62L, and MMP9 (40). Interestingly, lymph node and bone marrow homing of CLL cells from early and intermediate Rai stage patients has been shown to be impaired compared with normal B cells following their transfer into NOD/SCID mice due to defective LFA-1 and VLA-4 expression in a significant proportion of these patients (41). We did not observe a reduction in LFA-1 expression in our CLL cells (not shown), consistent with their unipaired adhesion to ICAM-1.

This is one of the first studies where the distribution of CXCR4, CCR7, and S1P1 has been analyzed *in situ* not only in CLL, but also in normal human lymphoid tissue. The role of these receptors has been extensively addressed in the mouse (42). Consistent with the role of CXCR4 in retaining

Published OnlineFirst August 17, 2015; DOI: 10.1158/0008-5472.CAN-15-0986

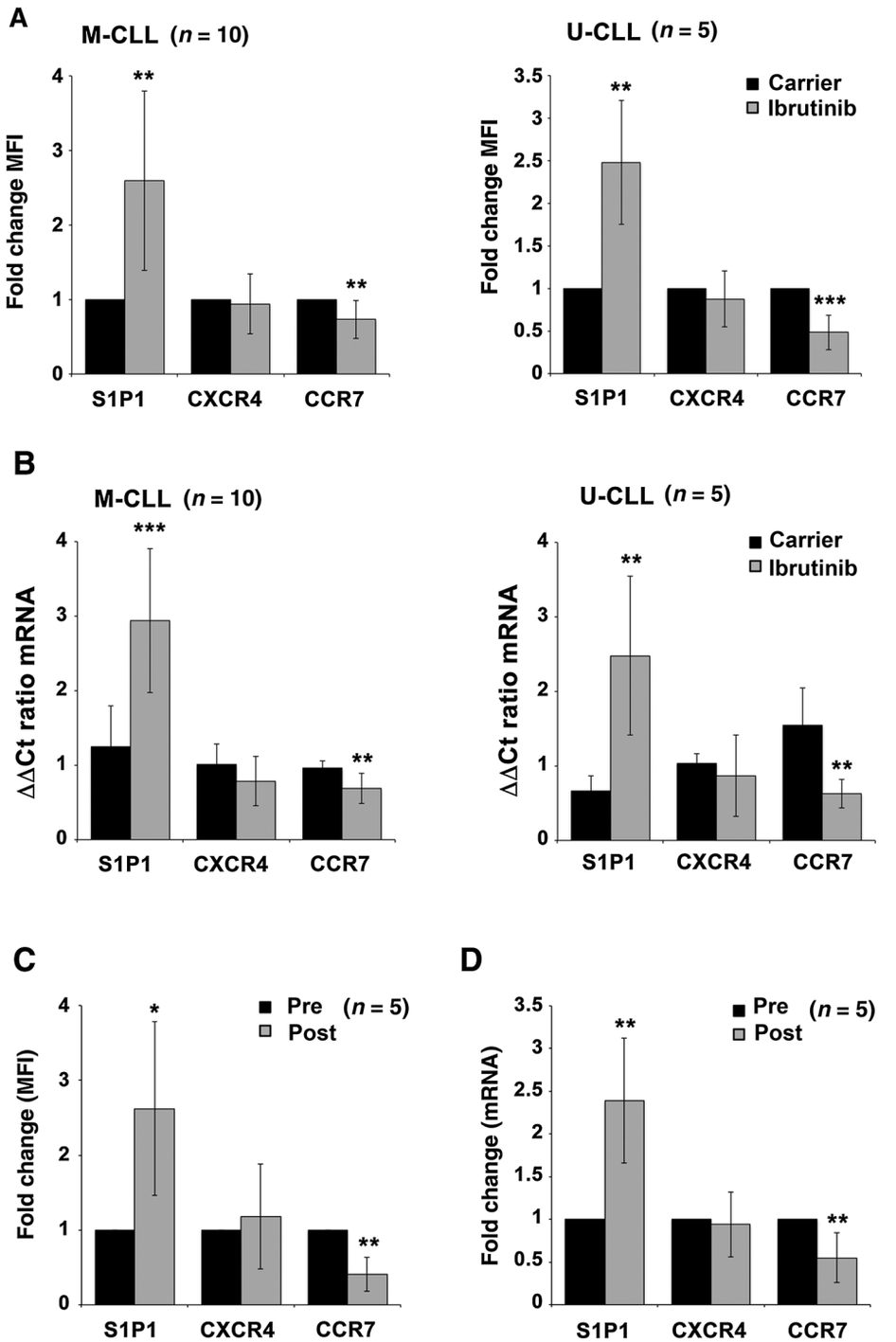

Figure 7.
Ibrutinib treatment promotes S1P1 and downregulates CCR7 expression in CLL cells. A, flow cytometric analysis of S1P1, CXCR4, and CCR7 on purified M-CLL or U-CLL B cells, treated with either DMSO (carrier) or 10 μmol/L ibrutinib for 48 hours. Data are expressed as fold MFI change in treated versus untreated samples. B, quantitative RT-PCR analysis of S1P1, CXCR4, and CCR7 mRNA in purified M-CLL or U-CLL B cells. The relative gene transcript abundance was determined on triplicate samples using the $\Delta\Delta C_t$ method (mean ± SD). C, flow cytometric analysis of S1P1, CXCR4, and CCR7 on purified peripheral B cells from 5 CLL patients with lymphoadenopathy, before (pre) and after (post) 4-month ibrutinib treatment. Data are expressed as fold MFI change in samples post- versus pretreatment. D, quantitative RT-PCR analysis of S1P1, CXCR4, and CCR7 on B cells from the same patients as in C. The relative gene transcript abundance was determined on triplicate samples using the $\Delta\Delta C_t$ method (fold change in samples post- vs. pretreatment). Error bars, SD. *, $P < 0.05$; **, $P < 0.01$; ***, $P < 0.001$.

centroblasts in GCs (25), normal reactive tonsillar tissue shows a strong CXCR4 immmunoreactivity. The CCR7 distribution is similar, with a strong GCs and T-cell zone immunoreactivity. In the mouse, CCR7 is downregulated once B cells enter lymph nodes, where CXCR5 takes over for follicular targeting, but re-expressed on antigen-engaged B cells to allow their movement to the T-cell zone (26). The CCR7 reactivity observed in human GCs is compatible with this scenario. Within lymphoid follicles, the S1P1 distribution pattern is complementary to that of CCR7/CXCR4, with strong immunoreactivity tightly restricted to mantle zone B cells. This result is consistent with a recent report describing the expression of S1P receptors in human B-cell subsets (39). The abundant S1P1 expression in mantle zone B cells suggests that, similar to mouse B cells, this receptor may

Published OnlineFirst August 17, 2015; DOI: 10.1158/0008-5472.CAN-15-0986

play a role in their migration towards the S1P-enriched follicle center (43). Interestingly, S1P1 expression has been recently reported to be reduced by BCR signaling (44), which might account for the lack of GC immunoreactivity and contribute to the S1P1 defect in CLL cells.

The notion that the homing and egress receptor imbalance contributes to retaining CLL cells in the stromal microenvironment is strongly supported by our finding that ibrutinib treatment, which promotes leukemic cell mobilization from SLOs, results in an increase in S1P1 expression, coupled to a reduction in CCR7. S1P1 expression is also upregulated in the presence of a Syk inhibitor (10), indicating that Btk and Syk participate in an inhibitory pathway controlling *S1P1* transcription. The apparent discrepancy of these results with those obtained by Till and colleagues showing that S1P1 expression, while downregulated by BCR signaling, is not affected by either Btk or Syk inhibitors (44), may be accounted for by the shorter duration of CLL cell treatment with these inhibitors. The fact that Btk couples BCR signaling to FoxO1 expression (45), which regulates CCR7 (46), could underlie the ability of ibrutinib to reduce its expression in CLL cells. Because Btk also participates in CXCR4 and CXCR5 signaling (12, 47), Btk inhibition would be predicted to also inhibit B-cell entry into SLOs and local traffic therein. Hence, the ibrutinib-related lymphocytosis in CLL is likely to result from the combined inhibition of leukemic cell homing to SLOs and bone marrow and their enhanced egress resulting from upregulation in *S1P1* expression.

Disclosure of Potential Conflicts of Interest

No potential conflicts of interest were disclosed.

Authors' Contributions

Conception and design: V. Martini, G. Semenzato, C.T. Baldari
Development of methodology: L. Patrussi, N. Capitani, C.T. Baldari
Acquisition of data (provided animals, acquired and managed patients, provided facilities, etc.): L. Patrussi, N. Capitani, V. Martini, M. Pizzi, V. Trimarco, F. Frezzato, F. Marino, G. Semenzato, L. Trentin
Analysis and interpretation of data (e.g., statistical analysis, biostatistics, computational analysis): L. Patrussi, N. Capitani, M. Pizzi, G. Semenzato, L. Trentin, C.T. Baldari
Writing, review, and/or revision of the manuscript: L. Patrussi, N. Capitani, M. Pizzi, G. Semenzato, L. Trentin, C.T. Baldari
Study supervision: G. Semenzato, C.T. Baldari

Acknowledgments

The authors thank Professor Massimo Rugge for advice on the IHC and Sonia Grassini for technical assistance.

Grant Support

This work was supported by grants from AIRC, MIUR (FIRB, PRIN), and ITT-Regione Toscana. N. Capitani is the recipient of FIRC fellowship.

The costs of publication of this article were defrayed in part by the payment of page charges. This article must therefore be hereby marked *advertisement* in accordance with 18 U.S.C. Section 1734 solely to indicate this fact.

Received April 13, 2015; revised July 10, 2015; accepted July 19, 2015; published OnlineFirst August 17, 2015.

References

1. Bono MR, Elgueta R, Sauma D, Pino K, Osorio F, Michea P, et al. The essential role of chemokines in the selective regulation of lymphocyte homing. Cytokine Growth Factor Rev 2007;18:33–43.
2. Kehrl JH, Hwang IY, Park C. Chemoattract receptor signaling and its role in lymphocyte motility and trafficking. Curr Top Microbiol Immunol 2009;334:107–27.
3. Kucia M, Jankowski K, Reca R, Wysoczynski M, Bandura L, Allendorf DJ, et al. CXCR4-SDF-1 signalling, locomotion, chemotaxis and adhesion. J Mol Histol 2004;35:233–45.
4. Comerford I, Harata-Lee Y, Bunting MD, Gregor C, Kara EE, McColl SR. A myriad of functions and complex regulation of the CCR7/CCL19/CCL21 chemokine axis in the adaptive immune system. Cytokine Growth Factor Rev 2013;24:269–83.
5. Burger JA, Gribben JG. The microenvironment in chronic lymphocytic leukemia (CLL) and other B cell malignancies: insight into disease biology and new targeted therapies. Semin Cancer Biol 2014;24: 71–81.
6. Packham G, Stevenson F. The role of the B-cell receptor in the pathogenesis of chronic lymphocytic leukaemia. Semin Cancer Biol 2010;20:391–9.
7. Lopez-Giral S, Quintana NE, Cabrerizo M, Alfonso-Perez M, Sala-Valdes M, De Soria VG, et al. Chemokine receptors that mediate B cell homing to secondary lymphoid tissues are highly expressed in B cell chronic lymphocytic leukemia and non-Hodgkin lymphomas with widespread nodular dissemination. J Leukoc Biol 2004;76:462–71.
8. Burkle A, Niedermeier M, Schmitt-Graff A, Wierda WG, Keating MJ, Burger JA. Overexpression of the CXCR5 chemokine receptor, and its ligand, CXCL13 in B-cell chronic lymphocytic leukemia. Blood 2007; 110:3316–25.
9. Capitani N, Patrussi L, Trentin L, Lucherini OM, Cannizzaro E, Migliaccio E, et al. S1P1 expression is controlled by the pro-oxidant activity of p66Shc and is impaired in B-CLL patients with unfavorable prognosis. Blood 2012;120:4391–9.
10. Borge M, Remes Lenicov F, Nannini PR, de los Rios Alicandu MM, Podaza E, Ceballos A, et al. The expression of sphingosine-1 phosphate receptor-1 in chronic lymphocytic leukemia cells is impaired by tumor microenvironmental signals and enhanced by piceatannol and R406. J Immunol 2014;193:3165–74.
11. Marchese A. Endocytic trafficking of chemokine receptors. Curr Opin Cell Biol 2014;27:72–7.
12. Patrussi L, Capitani N, Cannizzaro E, Finetti F, Lucherini OM, Pelicci PG, et al. Negative regulation of chemokine receptor signaling and B-cell chemotaxis by p66Shc. Cell Death Dis 2014;5:e1068.
13. Capitani N, Lucherini OM, Sozzi E, Ferro M, Giommoni N, Finetti F, et al. Impaired expression of p66Shc, a novel regulator of B-cell survival, in chronic lymphocytic leukemia. Blood 2010;115:3726–36.
14. Finetti F, Paccani SR, Riparbelli MG, Giacomello E, Perinetti G, Pazour GJ, et al. Intraflagellar transport is required for polarized recycling of the TCR/CD3 complex to the immune synapse. Nat Cell Biol 2009;11:1332–9.
15. Manders EM, Stap J, Brakenhoff GJ, van Driel R, Aten JA. Dynamics of three-dimensional replication patterns during the S-phase, analysed by double labelling of DNA and confocal microscopy. J Cell Sci 1992; 103:857–62.
16. Finetti F, Patrussi L, Masi G, Onnis A, Galgano D, Lucherini OM, et al. Specific recycling receptors are targeted to the immune synapse by the intraflagellar transport system. J Cell Sci 2014;127:1924–37.
17. Margadant C, Kreft M, de Groot DJ, Norman JC, Sonnenberg A. Distinct roles of talin and kindlin in regulating integrin alpha5beta1 function and trafficking. Curr Biol 2012;22:1554–63.
18. Patrussi L, Ulivieri C, Lucherini OM, Paccani SR, Gamberucci A, Lanfrancone L, et al. p52Shc is required for CXCR4-dependent signaling and chemotaxis in T cells. Blood 2007;110:1730–8.
19. Ludwig K, Fassan M, Mescoli C, Pizzi M, Balistreri M, Albertoni L, et al. PDCD4/miR-21 dysregulation in inflammatory bowel disease-associated carcinogenesis. Virchows Archiv 2013;462:57–63.
20. Damle RN, Wasil T, Fais F, Ghiotto F, Valetto A, Allen SL, et al. Ig V gene mutation status and CD38 expression as novel prognostic indicators in chronic lymphocytic leukemia. Blood 1999;94:1840–7.
21. Hamblin TJ, Davis Z, Gardiner A, Oscier DG, Stevenson FK. Unmutated Ig V (H) genes are associated with a more aggressive form of chronic lymphocytic leukemia. Blood 1999;94:1848–54.

22. Marchese A, Raiborg C, Santini F, Keen JH, Stenmark H, Benovic JL. The E3 ubiquitin ligase AIP4 mediates ubiquitination and sorting of the G protein-coupled receptor CXCR4. Dev Cell 2003;5:709–22.
23. Otero C, Groettrup M, Legler DF. Opposite fate of endocytosed CCR7 and its ligands: recycling versus degradation. J Immunol 2006;177: 2314–23.
24. Swat W, Fujikawa K. The Vav family: at the crossroads of signaling pathways. Immunol Res 2005;32:259–65.
25. Allen CD, Ansel KM, Low C, Lesley R, Tamamura H, Fujii N, et al. Germinal center dark and light zone organization is mediated by CXCR4 and CXCR5. Nat Immunol 2004;5:943–52.
26. Reif K, Ekland EH, Ohl L, Nakano H, Lipp M, Forster R, et al. Balanced responsiveness to chemoattractants from adjacent zones determines B-cell position. Nature 2002;416:94–9.
27. Hardtke S, Ohl L, Forster R. Balanced expression of CXCR5 and CCR7 on follicular T helper cells determines their transient positioning to lymph node follicles and is essential for efficient B-cell help. Blood 2005;106: 1924–31.
28. Byrd JC, Furman RR, Coutre SE, Flinn IW, Burger JA, Blum KA, et al. Targeting BTK with ibrutinib in relapsed chronic lymphocytic leukemia. New Engl J Med 2013;369:32–42.
29. de Rooij MF, Kuil A, Geest CR, Eldering E, Chang BY, Buggy JJ, et al. The clinically active BTK inhibitor PCI-32765 targets B-cell receptor- and chemokine-controlled adhesion and migration in chronic lymphocytic leukemia. Blood 2012;119:2590–4.
30. Cheng S, Ma J, Guo A, Lu P, Leonard JP, Coleman M, et al. BTK inhibition targets in vivo CLL proliferation through its effects on B-cell receptor signaling activity. Leukemia 2014;28:649–57.
31. Wodarz D, Garg N, Komarova NL, Benjamini O, Keating MJ, Wierda WG, et al. Kinetics of CLL cells in tissues and blood during therapy with the BTK inhibitor ibrutinib. Blood 2014;123:4132–5.
32. Till KJ, Lin K, Zuzel M, Cawley JC. The chemokine receptor CCR7 and alpha4 integrin are important for migration of chronic lymphocytic leukemia cells into lymph nodes. Blood 2002;99:2977–84.
33. Barretina J, Junca J, Llano A, Gutierrez A, Flores A, Blanco J, et al. CXCR4 and SDF-1 expression in B-cell chronic lymphocytic leukemia and stage of the disease. Ann Hematol 2003;82:500–5.
34. Burger JA, Burger M, Kipps TJ. Chronic lymphocytic leukemia B cells express functional CXCR4 chemokine receptors that mediate spontaneous migration beneath bone marrow stromal cells. Blood 1999;94: 3658–67.
35. Mohle R, Failenschmid C, Bautz F, Kanz L. Overexpression of the chemokine receptor CXCR4 in B cell chronic lymphocytic leukemia is associated with increased functional response to stromal cell-derived factor-1 (SDF-1). Leukemia 1999;13:1954–9.
36. Schaeuble K, Hauser MA, Rippl AV, Bruderer R, Otero C, Groettrup M, et al. Ubiquitylation of the chemokine receptor CCR7 enables efficient receptor recycling and cell migration. J Cell Sci 2012;125:4463–74.
37. Marchese A, Benovic JL. Agonist-promoted ubiquitination of the G protein-coupled receptor CXCR4 mediates lysosomal sorting. J Biol Chem 2001;276:45509–12.
38. Berlin I, Higginbotham KM, Dise RS, Sierra MI, Nash PD. The deubiquitinating enzyme USP8 promotes trafficking and degradation of the chemokine receptor 4 at the sorting endosome. J Biol Chem 2010;285: 37895–908.
39. Sic H, Kraus H, Madl J, Flittner KA, von Munchow AL, Pieper K, et al. Sphingosine-1-phosphate receptors control B-cell migration through signaling components associated with primary immunodeficiencies, chronic lymphocytic leukemia, and multiple sclerosis. J Allergy Clin Immunol 2014;134:420–8.
40. Davids MS, Burger JA. Cell Trafficking in Chronic Lymphocytic Leukemia. Open J Hematol 2012;3(S1).
41. Hartmann TN, Grabovsky V, Wang W, Desch P, Rubenzer G, Wollner S, et al. Circulating B-cell chronic lymphocytic leukemia cells display impaired migration to lymph nodes and bone marrow. Cancer Res 2009; 69:3121–30.
42. Cyster JG. Chemokines, sphingosine-1-phosphate, and cell migration in secondary lymphoid organs. Annu Rev Immunol 2005;23:127–59.
43. Cinamon G, Matloubian M, Lesneski MJ, Xu Y, Low C, Lu T, et al. Sphingosine 1-phosphate receptor 1 promotes B cell localization in the splenic marginal zone. Nat Immunol 2004;5:713–20.
44. Till KJ, Pettitt AR, Slupsky JR. Expression of Functional Sphingosine-1 Phosphate Receptor-1 Is Reduced by B Cell Receptor Signaling and Increased by Inhibition of PI3 Kinase delta but Not SYK or BTK in Chronic Lymphocytic Leukemia Cells. J Immunol 2015;194:2439–46.
45. Hinman RM, Bushanam JN, Nichols WA, Satterthwaite AB. B cell receptor signaling down-regulates forkhead box transcription factor class O 1 mRNA expression via phosphatidylinositol 3-kinase and Bruton's tyrosine kinase. J Immunol 2007;178:740–7.
46. Kerdiles YM, Beisner DR, Tinoco R, Dejean AS, Castrillon DH, DePinho RA, et al. Foxo1 links homing and survival of naive T cells by regulating L-selectin, CCR7 and interleukin 7 receptor. Nat Immunol 2009;10:176–84.
47. de Gorter DJ, Beuling EA, Kersseboom R, Middendorp S, van Gils JM, Hendriks RW, et al. Bruton's tyrosine kinase and phospholipase Cγ2 mediate chemokine-controlled B cell migration and homing. Immunity 2007;26:93–104.

Published OnlineFirst August 17, 2015; DOI: 10.1158/0008-5472.CAN-15-0986

Cancer Research
The Journal of Cancer Research (1916–1930) | The American Journal of Cancer (1931–1940)

AACR American Association for Cancer Research

Enhanced Chemokine Receptor Recycling and Impaired S1P1 Expression Promote Leukemic Cell Infiltration of Lymph Nodes in Chronic Lymphocytic Leukemia

Laura Patrussi, Nagaja Capitani, Veronica Martini, et al.

Cancer Res 2015;75:4153-4163. Published OnlineFirst August 17, 2015.